JÓVENES EN LA CIENCIA
REVISTA DE DIVULGACIÓN CIENTÍFICA

CFD MODELING OF HEAT SINKS UNDER REALISTIC OPERATING CONDITIONS

Joshua Acosta (1), Sergio Cano-Andrade (2)

1 Department of Mechanical Engineering, Massachusetts Institute of Technology, Cambridge, Massachusetts 02139, USA | Dirección de correo electrónico: ajoshua@mit.edu

2 Departamento de Ingeniería Mecánica, Universidad de Guanajuato, Salamanca, Guanajuato 36885, México | Dirección de correo electrónico: sergio.cano@ugto.mx

Resumen

La potencia de los circuitos integrados ha aumentado, lo que requiere que los intercambiadores de calor sean más pequeños y que remuevan mayores flujos de calor. Además, la mayoría de las fallas en los circuitos son resultado del calentamiento. En este artículo se presenta el análisis de un disipador de calor para el enfriamiento del procesador de una computadora usada en investigación. Agua dieléctrica es usada como fluido de trabajo en lugar de aire como lo hacen los disipadores convencionales actuales. Diferentes condiciones de operación para la computadora son simuladas al cambiar la razón del flujo volumétrico para estudiar el funcionamiento del disipador de calor. El modelo se simula en un programa comercial de CFD. La calidad de la malla se estudia usando un flujo de calor de 100 kW/m^2 aplicado en la base del disipador. Los resultados muestran que con 360,000 elementos se logra la independencia de la malla. Además, el uso de 360,000 elementos ayuda a reducir el tiempo de cómputo. Los resultados también muestran que el desempeño del disipador de calor se mejora al aumentar la razón de flujo volumétrico, obteniendo un incremento en la temperatura de salida del fluido de 9 K a 4.17X10^{-4} m^3/s.

Abstract

As the power density of integrated circuits has increased, requiring heat sinks to be smaller, they have to be capable of dissipating greater heat fluxes. However, the majority of integrated circuit failures result from thermal activated processes. In this paper, we present a heat sink for cooling the processor of a desktop computer used for research purposes. The heat sink uses a liquid as a working fluid as opposed to air like conventional heat sinks. Different operating conditions of the computer are simulated by changing the volumetric flow rate of the working fluid to analyze the performance of the heat sink under those operating conditions. The models are simulated using a commercial CFD program. Additionally, we study the mesh quality of the model using a heat flux of 100 kW/m^2 applied to the base of the heat sink. Results show that with 360,000 elements, grid independence is achieved. Furthermore, using 360,000 elements helps reduce computational time. Finally, the results illustrate that the thermal performance of the heat sink is improved at higher volumetric flow rates with a maximum outlet fluid temperature increase of 9 K at 4.17X10^{-4} m^3/s.

Keywords CFD modeling, heat sink, single-phase flow, electronic cooling

INTRODUCTION

Under normal operating conditions, computer components, (e.g. central processing unit), generate heat. Removing the waste heat is critical to maintaining the computer components within permissible operating conditions. Temporary malfunction or permanent failure can occur if components overheat. Most failure mechanisms within integrated circuits are thermally activated processes [1].

The development and miniaturization of integrated circuits has gradually resulted in greater power densities, as well as the requirement for more effective and compact cooling methods [2]. In 1981, Tuckerman and Pease [3] proposed the concept of microchannel heat sinks in order to meet the increasing cooling requirements for circuits. With a maximum substrate temperature increase of 71 oC, they illustrated the heat sink was capable of performing up to a power density of 790 W/cm2.

A microchannel heat sink consists of a parallel arrangement of fins and channels with a hydraulic diameter of 1 μm < Dh < 1 mm [4]. With the heat sink adjacent to the integrated circuit, the heat is transferred to the base of the heat sink via conduction. Heat is transferred away by flowing coolant through the channels. The reduction in the channel hydraulic diameter increases the heat transfer coefficient [3]. Jajja et al. [5] investigated four heat sinks with fin spacing of 0.2 mm, 0.5 mm, 1.0 mm, and 1.5 mm exposed to 325 W. They observed the lowest heat sink base temperature of 40.5 oC with the smallest fin spacing of 0.2 mm.

Computer components are commonly cooled with fans, as well as heat sinks. Liquids are an alternative to using air as the coolant fluid, where the most commonly used liquid is distilled water. The heat transfer coefficient in forced convection is greater with a liquid medium as opposed to air. Compact designs coupled with a high surface area to volume ratio are notable aspects of liquid-cooled microchannels [3]. However, microchannel heat sinks are also associated with higher-pressure drops, resulting in additional hydraulic pump power requirements [6].

The heat transfer rate of microchannel heat sinks is comparable to that of boiling heat transfer [7]. With a typical maximum operating temperature of 70 oC, integrated circuits can be maintained at admissible operating conditions by increasing the capability of heat sinks to remove high heat fluxes [8]. Conventional channels can dissipate up to 20 W/cm2. Microchannel heat sinks are capable of dissipating heat fluxes upwards of 1000 W/cm2, although an optimal balance between heat transfer gains and a pressure drop penalty should be closely assessed [6].

MATERIALS AND METHODS

Geometry of the Heat Sink

The device studied in this paper is a nickel composition microchannel heat sink, and is shown in Figure 1a. The water block consists of 52 channels, where each channel is approximately 0.29 mm in width and 1.5 mm in height. As seen in Figure 1b, the jet plate slot is perpendicular to the flow direction. The lengthwise slit in the jet plate concurrently directs water into all 52 channels. At the center of each channel, the water flow path diverges into two streams, which flow to the perimeter pathway of the water block and then join at the outlet port as shown in Figure 1c. The water block cover including the jet plate and the outlet port are also depicted in Figure 1c.

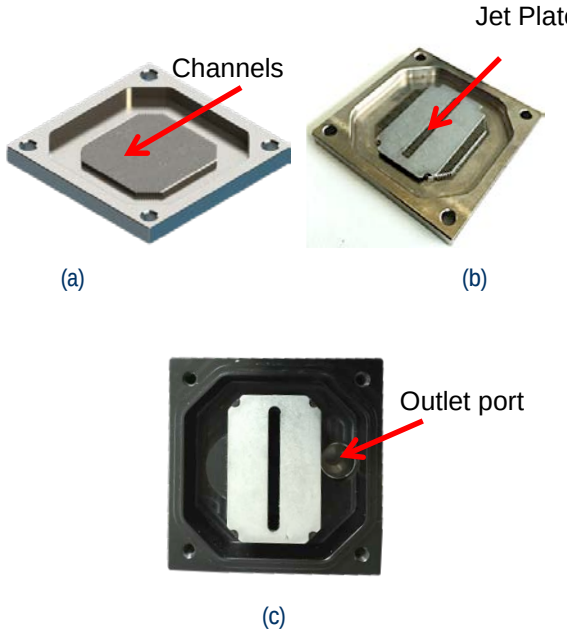

FIGURE 1: (a) SolidWorks Rendering of the heat sink, (b) picture of the water block with the jet plate placed over the channels, and (c) picture of the water block cover.

Computational Model Configuration

A total of three cases were evaluated with the CFD program ANSYS Fluent®. The software Gambit® is used to construct and mesh the model geometry. ANSYS Fluent® solves the continuity equation,

$$\vec{\nabla}\cdot(\rho\vec{u})=0 \quad (1)$$

the momentum equation in the three dimensions,

$$(\vec{u}\cdot\vec{\nabla})\rho\vec{u}=-\vec{\nabla}P+\vec{\nabla}(\mu\vec{\nabla}\cdot\vec{u}) \quad (2)$$

and the energy equation,

$$\rho C_p(\vec{u}\cdot\vec{\nabla}T)=k\vec{\nabla}\cdot(\vec{\nabla}T) \quad (3)$$

where $\vec{\nabla}$ is the Nabla operator, $\vec{u}$ is the velocity, P is the pressure, and ρ is the density of the mixture.

Convergence is said to occur when residuals levels for the continuity and momentum equations reach a value of 1X10-5 and a value below 1X10-8 for the energy equation.

For all different cases, a spatially and temporarily constant heat flux of 100 kW/m2 is applied to the base of the heat sink. Water is used as a working fluid with an inlet temperature of 293 K. The inlet volumetric flow rates were determined based upon the minimal, mean, and maximal volumetric flow rates of water-cooling pumps in the market. From then the three constant inlet water velocities were determined. The volumetric flow rates, inlet velocities, and water pump specifications are provided in Table 1.

TABLE 1. Volumetric flow rates and corresponding inlet water velocities for various water pumps.

Manufacturer	Model	Volumetric Flow Rate [m^3/s]	Inlet Water Velocity [m/s]
Alphacool	DC-LT	$3.33X10^{-5}$	0.80
Koolance	PMP-300	$1.17X10^{-4}$	2.80
Alphacool	VPP-Single	$4.17X10^{-4}$	9.99

A grid independence analysis is developed, where three mesh qualities, i.e., coarse, refined, and highly refined, are used. The three mesh qualities are comprised of 316,600 elements, 546,200 elements, and 1,081,000 elements, respectively. In particular, the cell aspect ratio was enhanced near the microchannel walls in order to better characterize the complexity of the boundary layer. Enlarged views of the three mesh qualities are depicted in Figure 2. For all three mesh cases, boundary and operating conditions remained unaltered, and a volumetric flow rate of 1.17X10-4 m3/s was used.

Computational Model Parameters and Assumptions

Due to its symmetrical design, only half of the heat sink region was simulated in order to reduce computational resources and time of simulation. The heat sink model in Gambit® is depicted in Figure 3. There is still a debate to determine whether macro-scale thermo-fluids theory is applicable to the analysis of the thermo-hydraulic performance of microchannel heat sinks [8], since molecular and continuum effects become more important in micro-scale flow [3]. Although there is yet to be an agreement on the pertinence of macro-scale theory in micro-scale fluid dynamics, this numerical simulation model is in accord with macro-scale theory and uses the following assumptions: (a) steady state conditions, (b) laminar flow, (c) single-phase flow, (d) incompressible flow, (e) constant fluid properties, and (f) radiation heat transfer is negligible.

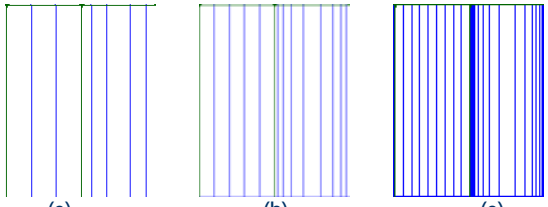

FIGURE 2: Different mess qualities for the model: (a) coarse mesh, (b) refined mesh, and (c) highly refined mesh.

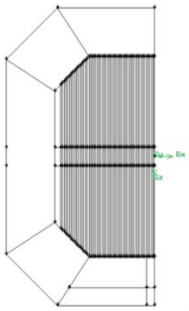

FIGURE 3: Model in Gambit® showing half of the heat sink geometry.

RESULTS AND DISCUSSION

Grid Independence Analysis

The temperature profile for three models composed of different mesh qualities is depicted in Figure 4. It is observed that there is no large deviation among the results of the three different mesh qualities, despite the highly refined mesh having 3.4 times as many elements as the coarse mesh. The temperature profile of the mesh consisting of 532,200 elements is indistinguishable from the mesh of 1,081,000 elements. The simulation using 532,200 elements takes approximately 35 minutes to complete, whereas, the simulation using 1,081,000 elements takes about 480 minutes. Therefore, computational load and time is reduced significantly by using a less refined mesh. Table 2 summarizes the numerical results of the heat sink simulation comprised of three different mesh qualities.

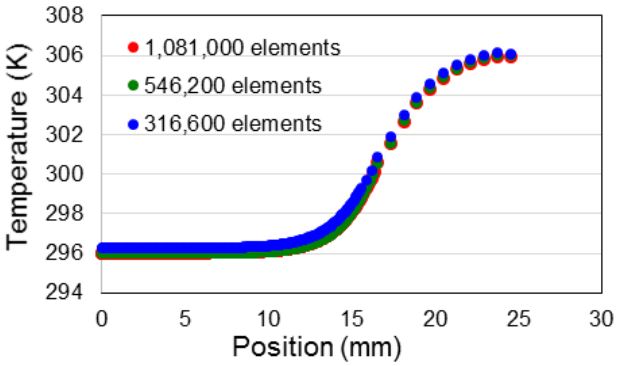

FIGURE 4: Temperature profile of the heat sink evaluated with three different mesh qualities.

TABLE 2. Summary of the results for the three different mesh quality cases.

Number of Elements	Maximum Temperature (K)		ΔT (K)	ΔP (kPa)
	Material		Material	
	Nickel	Water	Water	
316,600	306.99	296.20	3.2	312.34
546,200	306.91	297.81	4.81	317.40
1,081,000	306.84	298.66	5.66	324.37

Performance at Different Operating States

For the following cases, a total of 112.85 W is transferred through the base of the microchannel heat sink. It is critical for the region of the heat exchanger directly in contact with the integrated circuits, the heat sink base, to provide uniform cooling such that thermal spreading resistance is minimized. The temperature, velocity, and pressure profiles for the three different volumetric flow rates (see Table 1) are depicted in Figures 5, 6, and 7. An increase in the volumetric flow rate results in a greater pressure drop, in addition, the maximum temperatures of both the nickel base and fluid decrease. This is in line with Darcy's law, where the pressure drop is proportional to the square of the fluid velocity. The experimental results presented by Jajja et al. [5] are in accordance as well. In all three cases, there are localized hot spots situated at the corner edges of the heat sink base. The base temperature also increases with distance from the inlet ports. As Philips Richard explained [7], the surface temperature increases with distance from the channel entrance because the coolant temperature rises; as a result, the heat transfer coefficient decreases. Overall, the heat sink exhibited improved thermal performance at greater volumetric flow rates at the expense of an increase in pressure. Table 3 summarizes the numerical results of the heat sink operating at three different volumetric flow rates.

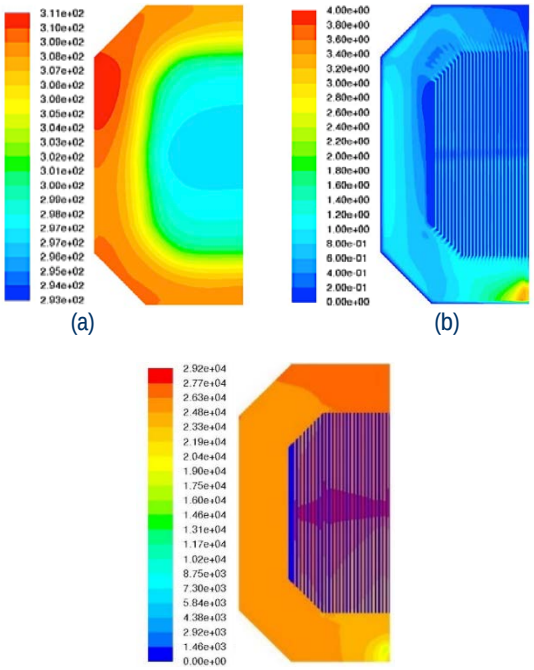

(a) (b) (c)

FIGURE 5: Results for the heat sink operating at a volumetric flow rate of 3.33X10^{-5} m^3/s: (a) temperature contour, (b) velocity contour, and (c) pressure contour.

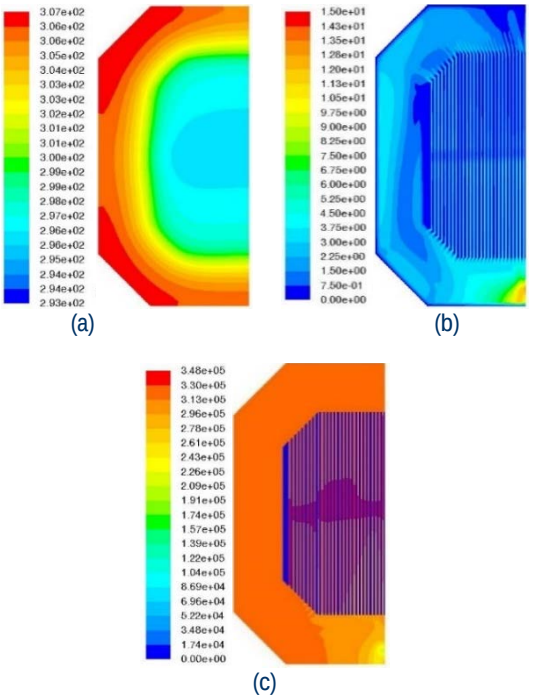

(a) (b) (c)

FIGURE 6: Results for the heat sink operating at a volumetric flow rate of 1.17X10^{-4} m^3/s: (a) temperature contour, (b) velocity contour, and (c) pressure contour.

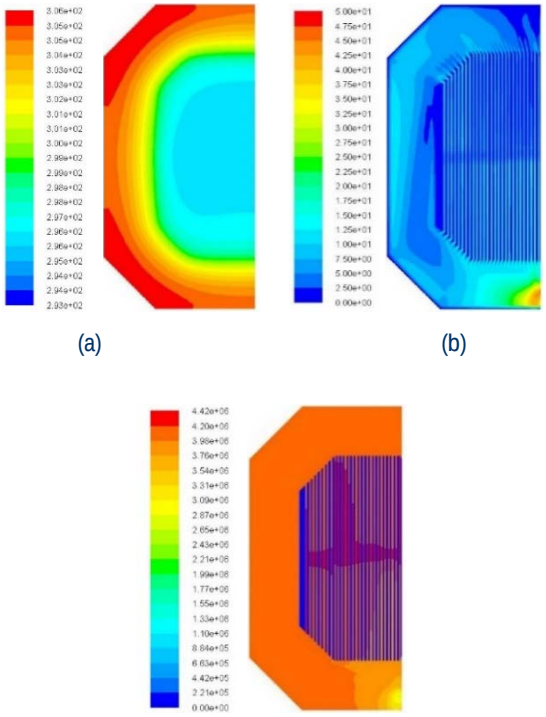

(a) (b) (c)

FIGURE 7: Results for the heat sink operating at a volumetric flow rate of 4.17X10^{-4} m^3/s: (a) temperature contour, (b) velocity contour, and (c) pressure contour.

TABLE 3. Summary of the results for the three different volumetric flow rates for the working fluid.

Volumetric Flow Rate [m³/s]	Maximum Temperature (K)		ΔT (K)	ΔP (kPa)
	Material		Material	
	Nickel	Water	Water	
3.33X10^{-5}	310.83	301.62	8.62	268.15
1.17X10^{-4}	306.91	297.81	4.81	317.40
4.17X10^{-4}	305.90	295.73	2.73	394.68

CONCLUSIONS

The study of a heat sink under three different operating conditions is presented. The study is developed using a commercial CFD software. The heat sink was subjected to 100 kW/m2. The heat

sink demonstrated better thermal performance operating at higher volumetric flow rates. Furthermore, there are localized hot spots on the heat sink base, which increase the thermal spreading resistance of the heat exchanger and can possibly lead to non-uniform cooling. The maximum substrate temperature increase is 9 K at a volumetric flow rate of 4.17X10-5 m3/s. With this heat sink, an integrated circuit rated at 85 W would be easily maintained at permissible operating temperatures with a 1.33 factor of safety. For further research, the model could be simulated using additional volumetric flow rates and additional heat fluxes in order to determine the optimal operating parameters for this particular heat sink.

ACKNOWLEDGMENTS

The authors are grateful to VERANOS UG 2015 for the opportunity to participate in this event. J.A. is also grateful to DINPO-UG for financial support, and to Carlos Ulises Gonzalez for providing advice and fruitful discussions during the completion of this work.

REFERENCES

[1] Tuckerman, D. B., and Pease, R. F. (1982) Ultrahigh thermal conductance microstructures for cooling integrated circuits, IEEE 32nd Electronics Components Conference Proc., 145-149.

[2] Gongnan, X., Zhiyong, C., Bengt, S., and Weihong, Z. (2013). Numerical predictions of the flow and thermal performance of water-cooled single-layer and double-layer wavy microchannel heat sinks. Numerical Heat Transfer, Part A: Applications, 63(3), 201-225.

[3] Tuckerman, D. B., & Pease, R. F., (1981), High Performance Heat Sinking for VLSI, IEEE Electronic Device Letters, Vol. EDL-2 No. 5.

[4] Gad-el-Hak M. (2006). MEMS: Introduction and Fundamentals. 2nd Edition, CRC Press, Taylor & Francis Group, Boca Raton, FL, Chap. 10.

[5] Jajja S. A., Ali, W., Ali, H. M., and Ali, A. M. (2014). Water cooled minichannel heat sinks for microprocessor cooling: effect of fin spacing. Applied Thermal Engineering, 64(1),76-82.

[6] Dixit T., Ghosh I. (2015). Review of micro- and mini-channel heat sinks and heat exchangers for single phase fluids. Renewable and Sustainable Energy Reviews, 41, 1298-1311.

[7] Phillips, J. R.. (1988). Microchannel heat sinks. The Lincoln Laboratory Journal, 1(1), 31-48.

[8] Rubio-Jimenez C. A., Rubio-Arana J. C., Guerrero-Hernandez A., & Kandlikar S. (2009). Natural patterns applied to the design of microchannel heat sinks. Proceedings of the ASME 2009 International Mech. Engineering Congress and Exposition.